

https://doi.org/10.11646/zootaxa.4554.1.10  
http://zoobank.org/urn:lsid:zoobank.org:pub:1E207D13-8863-4272-8C52-8C6E61F890D6

## A New Species of the *Graphium (Pazala) mandarinus* Group from Central Vietnam (Lepidoptera: Papilionidae)

SHAO-JI HU<sup>1,2</sup>, FABIEN L. CONDAMINE<sup>3</sup>, ALEXANDER L. MONASTYRSKII<sup>4</sup> & ADAM M. COTTON<sup>5,6</sup>

<sup>1</sup>*Yunnan Key Laboratory of International Rivers and Transboundary Eco-security, Yunnan University, Kunming, 650500, China*

<sup>2</sup>*Institute of International Rivers and Eco-security, Yunnan University, Kunming, 650500, China*

<sup>3</sup>*CNRS, UMR 5554 Institut des Sciences de l'Evolution de Montpellier, Université de Montpellier, Place Eugène Bataillon 34095 Montpellier, France*

<sup>4</sup>*Fauna & Flora International, Vietnam Programme, Hanoi, Vietnam*

<sup>5</sup>*86/2 Moo 5, Tambon Nong Kwai, Hang Dong, Chiang Mai, Thailand*

<sup>6</sup>*Corresponding author. E-mail: adamcot@cscoms.com*

### Abstract

The *Graphium (Pazala) mandarinus* group was recently defined and the status of taxa as well as the number of species was revised. We report here the discovery of a new species from Kon Tum plateau of the Truong Son (Annamite) Range of Central Vietnam, which we describe based on morphological and molecular evidence. Molecular phylogeny shows that the new taxon, *G. (P.) wenlingae* Hu, Cotton & Monastyrskii sp. nov., is sister to *G. (P.) daiyuanae* Hu, Zhang & Cotton, 2018 plus *G. (P.) confucius* Hu, Duan & Cotton, 2018. Molecular dating analysis further suggests that this new species diverged from its sister clade in the Pliocene (~3.5 million years ago). The new taxon constitutes the eighth and southernmost species of the *mandarinus* group.

**Key words:** *Pazala, mandarinus*-group, new species, Vietnam, Leptocircini

### Introduction

The *Graphium (Pazala) mandarinus* group was defined by Hu *et al.* (2018) with the discovery of five cryptic species among the two originally recognised species (Racheli & Cotton 2009). The main distinguishing character of the *mandarinus* group is the two discal black bands on the hindwing underside twisted into an “8”-shaped pattern, resembling a pair of glasses in appearance (Hu *et al.* 2018).

Shortly after the publication of the *mandarinus* group work (Hu *et al.* 2018) the authors of the present study received three specimens of *Pazala* swallowtails from two localities of Central Vietnam. Two specimens caught in 1998 were found in the collection of the Vietnam Forest Museum (VFM), Hanoi, bringing the total known number of specimens to 3♂♂ and 2♀♀. The external appearances of these specimens are similar to *G. (P.) daiyuanae* Hu, Zhang & Cotton, 2018, while several characters exhibit stable differences. After a careful examination of both external morphological characters and structure of male and female genitalia, along with analyses of molecular phylogeny and genetic distances, the specimens from Central Vietnam are believed to be a distinct species and are described herein.

### Materials and methods

**Taxon sampling.** Five specimens of the new taxon collected from Central Vietnam were examined in the present study. All samples were used for morphological comparison, while only three freshly collected samples, from 2017 and 2018, were used for molecular analyses. Specimens listed in Appendix 1 of Hu *et al.* (2018) and their DNA data are also integrated in this study.

**Morphological comparison.** Specimens were spread for examination, with the scent scales on their hindwings exposed.

Spread specimens were photographed using a Fujifilm S8600 digital camera (Fujifilm, Japan) with medium grey background. Photos were adjusted using Adobe Photoshop CS (Adobe, USA). Diagnostic characters of the new taxa were also denoted using Adobe Photoshop CS. For comparison between taxa, the lengths of forewing were measured to 0.5 mm precision. Average lengths and the standard deviations were also calculated when  $n \geq 3$ .

To observe the male and female genitalia, the abdomen was taken from the specimen and placed into a 1.5 mL microcentrifuge tube, and 1 mL water was added to the abdomen to rehydrate the tissue at 50 °C for 30 min, then 1 mL 10% sodium hydroxide solution was used to digest soft tissue at 70 °C for 1 h. The treated abdomen was neutralised with 2% acetic acid and then dissected in a water-filled Petri dish under the stereoscope to remove residual tissues, scales, and hair. The genitalia were then transferred to 80% glycerol for 12 h to render them transparent. Photographs were taken with a Nikon DMX1200 digital camera (Nikon, Japan) mounted on a Nikon SMZ1500 stereoscope (Nikon, Japan) and automatically stacked using Helicon Focus 3.2 (Helicon Software, USA). The distance between socii of male genitalia is a useful morphometric character helpful to distinguish species (Koiwaya 1993); therefore this distance was measured to 0.2 mm precision for all dissected male genitalia. After observation and photography, all parts of the genitalia were fixed on a glue card and pinned with the specimen.

Terminology of genitalia follows Hu *et al.* (2018) and wing venation is as per Smith & Vane-Wright (2001).

**Molecular work.** For the three fresh specimens, one or two legs (except forelegs) on the same side were extracted, homogenised in protease buffer containing 100 μL STE (10 mmol/L Tris-HCl, 1 mmol/L EDTA, 100 mmol/L NaCl, pH = 8.0) and 2 μL Proteinase K (20 mg/mL) (O'Neill *et al.* 1992). Homogenised samples were treated at 37 °C incubation for 15 min to rehydrate the tissue and then at 95 °C incubation for 10 min to lyse the tissue. The supernatant was recovered through centrifugation at 6,000g and used directly as DNA template in polymerase chain reactions (PCR).

The PCR reaction was executed in a 25 μL system by using TaKaRa Ex *Taq* Kit (TaKaRa Biotechnology Co., Ltd., Dalian, China) that contained 2.5 μL of 10× PCR buffer, 2.0 μL of MgCl<sub>2</sub> (25 mmol/L), 2.0 μL of dNTP mixture (2.5 mmol/L each), 0.25 μL of *Taq* DNA polymerase (5 U/μL), and 0.5 μL of each of forward and reverse primers (20 μmol/L). We sequenced the mitochondrial barcode COI (cytochrome c oxidase subunit I, *cox1*) with the following primers LCO1490 (5'- GGT CAA CAA ATC ATA AAG ATA TTG G-3') and HCO2198 (5'- TAA ACT TCA GGG TGA CCA AAA AAT CA-3') (Folmer *et al.* 1994). The thermal profile of PCR consisted of an initial denaturation at 95 °C for 3 min; 30 cycles of denaturation at 94 °C for 1 min, annealing at 50 °C for 1 min, and elongation at 72 °C for 1 min; then a final elongation at 72 °C for 5 min. Sequences were obtained by using an ABI Prism 3730 sequencer (Applied Biosystems, California, USA).

**Phylogenetic analyses.** Raw sequences were proofread and aligned using Clustal W (Thompson *et al.* 1994) in BioEdit 7.0.9 (Hall 1999), and any sequence containing double peaks in the chromatograms was strictly excluded. The product sequences were checked by BLAST against the genomic references and nucleotide collection in NCBI. Amino acid translation was realised with the invertebrate mitochondrial criterion in MEGA 6.0 (Tamura *et al.* 2013) to detect possible *Numts* (nuclear copies of mtDNA fragments). A search for nonsynonymous mutations, in-frame stop codons, and indels was carried out to further minimise the existence of cryptic *Numts* (Song *et al.* 2008; Bertheau *et al.* 2011). Sequences used in the present study, including those derived from Hu *et al.* (2018), were listed in Table 1.

The phylogeny was reconstructed using the Bayesian Inference (BI) method as implemented in MrBayes 3.2.6 (Ronquist *et al.* 2012), with the most appropriate partition scheme recovered by PartitionFinder 2.1.1 (Lanfear *et al.* 2017) using the *unlinked* branch lengths and the *greedy* algorithm. We used the partitioning scheme and among-site rate variation suggested by PartitionFinder but instead of selecting one substitution model *a priori*, we used reversible-jump Markov Chain Monte Carlo (rj-MCMC) to allow sampling across the entire substitution rate model space (Huelskenbeck *et al.* 2004). BI analyses consisted of three independent runs, each with eight rj-MCMC running for 10 million generations (sampled every 1000<sup>th</sup> generation) to calculate the clade posterior probabilities (PP).

Maximum likelihood analyses were also carried out using IQ-TREE 1.6.8 (Nguyen *et al.* 2015). The dataset was partitioned as determined by PartitionFinder. The corresponding substitution models were searched using the Auto function on the IQ-TREE based on the corrected Akaike information criterion. We performed 1000 ultrafast bootstrap replicates (Minh *et al.* 2013) to investigate nodal support across the topology considering bootstrap values (BV)  $\geq 95$  as strongly supported.

As in Hu *et al.* (2018), we used an individual of *Iphiclidess podalirius* (Linnaeus, 1758) and of *Lamproptera*

*megei* (Zinken, 1831), because we found that tree topology and node support were improved when using outgroup species that branched before *Pazala*. We reconstructed the phylogeny for a dataset containing the currently recognised species of *Pazala* (*sensu* Hu *et al.* 2018) in an attempt to obtain an overall phylogenetic framework for the subgenus and to produce phylogenetic relationships among the focal taxon in the present study (*G. wenlingae* sp. nov.).

Phyletic properties of each taxon in the *mandarinus* group were assessed using an online tool, Monophylizer (Mutranen *et al.* 2016; <http://monophylizer.naturalis.nl/>). Taxa identified as monophyletic were treated as good species or subspecies, while those identified as paraphyletic (the terms ‘entangled’ and ‘tanglees’ described by Mutranen *et al.* 2016 were adopted to refer to such taxa in this study) were further analysed using morphological characters and geographical ranges.

**Molecular dating.** To estimate divergence times and infer their 95% credibility intervals (CI), we performed Bayesian relaxed-clock analyses using MrBayes. For these analyses, we relied on the partitioning scheme and all the MrBayes settings as determined above. Dating analyses were realized with three independent runs for 20 million generations with sampling tree every 2,000 generations. We used the autocorrelated clock model of Thorne & Kishino (2002, noted TK02 in MrBayes) for two reasons. First, the autocorrelated model is more appropriate for our dataset because the rate along a given branch is more similar to its parent branch than a branch chosen at random, though autocorrelation models differ in the degree to which they restrict rate variation between parent and daughter branches (Thorne *et al.* 1998; Thorne & Kishino 2002). Second, Lepage *et al.* (2007) and Rehm *et al.* (2011) showed that the autocorrelated clock model generally offers the best fit, as compared to the uncorrelated model and a strict molecular clock model.

Calibration priors are based on the time-calibrated tree of Papilionidae (Condamine *et al.* 2012). We set four secondary calibrations using a (conservative) uniform prior with bounded by the minimum and maximum ages of the 95% CI of the divergence times (a normal prior is not recommended, Schenk 2016). We could not use fossils in this study because the three fossils do not belong to the subfamily Papilioninae (Condamine *et al.* 2012). We calibrated the following nodes: (i) the root of the tree (crown of Leptocircini) set between 27.6 and 43.4 Ma; (ii) the crown between *Iphiclides* and *Lamproptera* set between 20.8 and 35.5 Ma; (iii) the crown of the genus *Graphium* set between 21.2 and 35.7 Ma; and (iv) the crown of the subgenus *Graphium* set between 14.4 and 29.7 Ma.

For all Bayesian runs (phylogenies and dating), convergence was ensured by checking average deviation of split frequencies (ADSF), potential scale reduction factor (PSRF) values, effective sample size (ESS) of all parameters, and by plotting log-likelihood of samples against number of generations in Tracer 1.6. To reach good convergence, the runs must have values of ADSF approaching zero, PSRF close to 1.00 and ESS above 200. Bayesian consensus trees were obtained using the 25% burn-in criterion (Ronquist *et al.* 2012), and the remaining samples were used to generate a 50% majority rule consensus tree.

All phylogenetic and dating analyses were performed on the computer cluster CIPRES Science Gateway (Miller *et al.* 2015), using BEAGLE (Ayres *et al.* 2012) with default parameters.

## Results

**Molecular analyses.** We obtained 658 base pairs of the mitochondrial gene COI for three specimens of *G. wenlingae* sp. nov., which were added to the data available for the *mandarinus* group (Hu *et al.* 2018). The partitioning analyses indicated that the COI gene should be divided into three partitions corresponding to each codon position. PartitionFinder further suggested that GTR model with invariable site and Gamma distribution should be applied, but we used the reversible-jump MCMC to explore a broader range of substitution models during the analyses. The Bayesian analyses showed that the new taxon, *G. (P.) wenlingae* sp. nov., is sister to *G. (P.) daiyuanae* + *G. (P.) confucius* (Figure 1). Topology and monophyly of other clades of the updated Bayesian tree of the *mandarinus* group remains the same as that reported by Hu *et al.* (2018), except *G. (P.) mandarinus stilwelli* was entangled with both *G. (P.) mandarinus fangana* and *G. (P.) mandarinus mandarinus* (Figure 1; Table 2).

The Bayesian molecular dating analysis estimated very similar divergence times as those reported in Hu *et al.* (2018). The entire *mandarinus* group split from its ancestor at 17.94 Ma (95% CI: 11.21–25.1 Ma) (Figure 2). Three clades, *G. (P.) wenlingae* sp. nov. + *G. (P.) daiyuanae* + *G. (P.) confucius*, *G. (P.) sichuanica* + *G. (P.) hoeneanus*, and the entire *G. (P.) mandarinus* clade formed a trichotomy in the dating tree, with a node age at 5.73 Ma (95% CI: 2.65–10.15 Ma) (Figure 2). The new taxon, *G. (P.) wenlingae* sp. nov., split from its ancestor at 3.54 Ma (95% CI: 1.31–7.11 Ma).

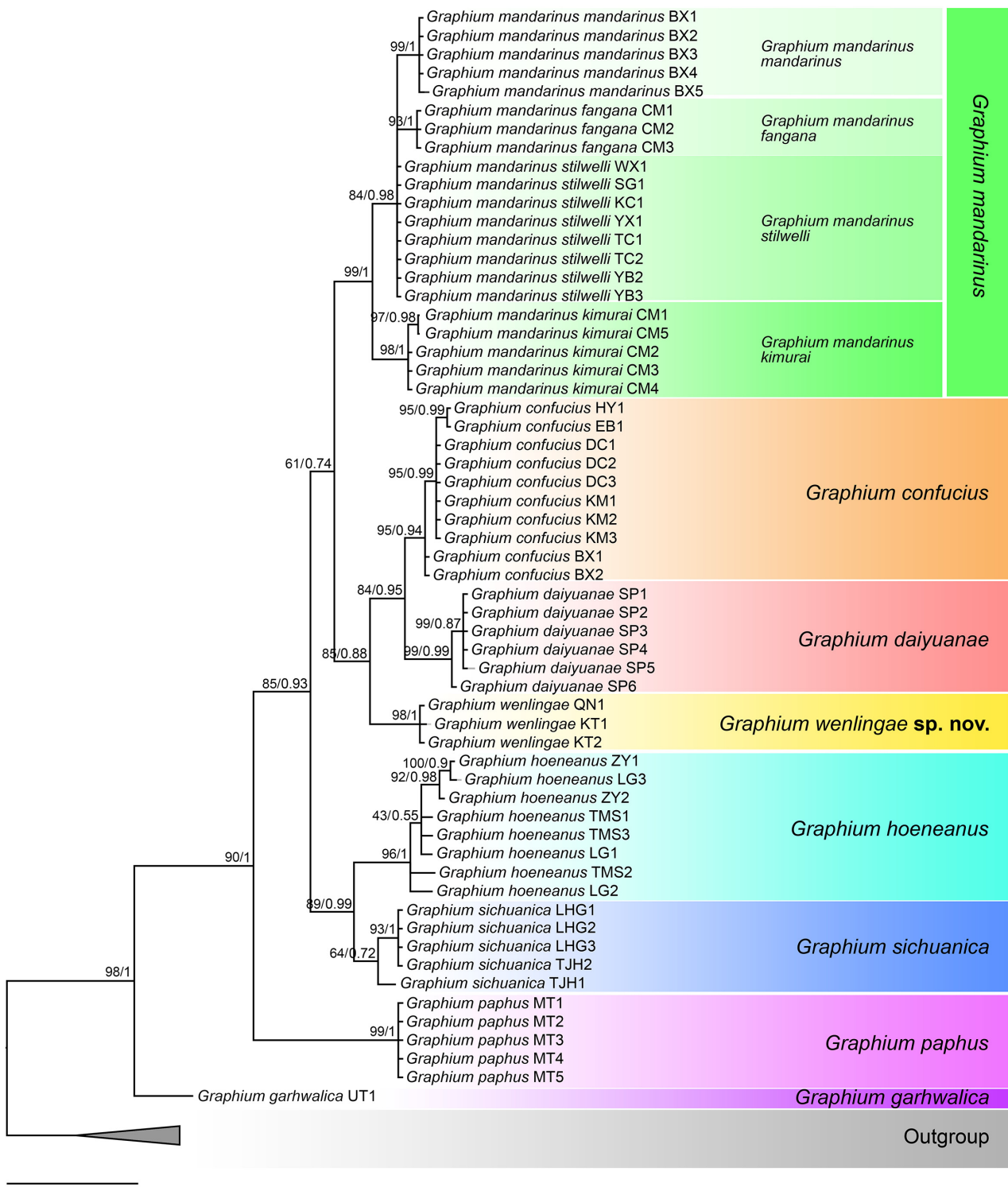


**FIGURE 1.** Bayesian phylogenetic tree of *Graphium (Pazala) mandarinus* group, with outgroups collapsed. Coloured rectangles delineate the species and subspecies, values at nodes indicate the bootstrap value/posterior probability.

Kimura 2-parameter (K2P) genetic distance (Table 3) computed between *G. (P.) wenlingae* sp. nov. and *G. (P.) daiyuanae* was 2.38%, and that between *G. (P.) wenlingae* sp. nov. and *G. (P.) confucius* was 2.24%, both greater than the K2P distance between *G. (P.) daiyuanae* and *G. (P.) confucius* (1.71%). The K2P distances between *G. (P.) wenlingae* sp. nov. and other morphologically similar taxa, namely *G. (P.) mandarinus kimurai*, *G. (P.) mandarinus fangana*, and *G. (P.) mandarinus stilwelli*, all exceeded 3%. It is also noticeable that the K2P distance between *G. (P.) wenlingae* sp. nov. and *G. (P.) sichuanica* was greater than that between *G. (P.) wenlingae* sp. nov. and *G. (P.) hoeneanus*.

**TABLE 1.** Specimens used in molecular analysis with GenBank accession numbers, accession numbers shared between samples with the same *cox1* sequence.

Taxon (sample code)	Locality	Accession No.
<i>G (P.) garhwalica</i> (UT1)	Joshimath, Uttarakhand, India	MG197758
<i>G (P.) paphus</i> (MT1–5)	Metok, Tibet, China	MG197757
<i>G (P.) sichuanica</i> (LHG1–3)	Laohegou, Sichuan, China	MG197767
<i>G (P.) sichuanica</i> (TJH1)	Tangjiahe, Sichuan, China	MG197768
<i>G (P.) sichuanica</i> (TJH2)	Tangjiahe, Sichuan, China	MG197767
<i>G (P.) hoeneanus</i> (ZY1)	Ziyuan, Guangxi, China	MG197762
<i>G (P.) hoeneanus</i> (ZY2)	Ziyuan, Guangxi, China	MG197763
<i>G (P.) hoeneanus</i> (LG1)	Lingui, Guangxi, China	MG197764
<i>G (P.) hoeneanus</i> (LG2)	Lingui, Guangxi, China	MG197765
<i>G (P.) hoeneanus</i> (LG3)	Lingui, Guangxi, China	MG197766
<i>G (P.) hoeneanus</i> (TMS1)	W. Tianmu Shan, Zhejiang, China	MG197759
<i>G (P.) hoeneanus</i> (TMS2)	W. Tianmu Shan, Zhejiang, China	MG197760
<i>G (P.) hoeneanus</i> (TMS3)	W. Tianmu Shan, Zhejiang, China	MG197761
<i>G (P.) wenlingae</i> sp. nov. (KT1)	Ngoc Linh, Kon Tum, Vietnam	MH892413
<i>G (P.) wenlingae</i> sp. nov. (KT2)	Ngoc Linh, Kon Tum, Vietnam	MH892412
<i>G (P.) wenlingae</i> sp. nov. (QN1)	Tay Giang, Quang Nam, Vietnam	MH892412
<i>G (P.) daiyuanae</i> (SP1–4)	Sapa, Lao Cai, Vietnam	MG197773
<i>G (P.) daiyuanae</i> (SP5)	Sapa, Lao Cai, Vietnam	MG197774
<i>G (P.) daiyuanae</i> (SP6)	Sapa, Lao Cai, Vietnam	MG197775
<i>G (P.) confucius</i> (HY1)	Hanyuan, Sichuan, China	MG197770
<i>G (P.) confucius</i> (EB1)	Ebian, Sichuan, China	MG197770
<i>G (P.) confucius</i> (BX1–2)	Baoxing, Sichuan, China	MG197769
<i>G (P.) confucius</i> (DC1, DC3)	Dongchuan, Yunnan, China	MG197771
<i>G (P.) confucius</i> (DC2)	Dongchuan, Yunnan, China	MG197772
<i>G (P.) confucius</i> (KM1–3)	Kunming, Yunnan, China	MG197771
<i>G (P.) mandarinus kimurai</i> (CM1)	Doi Inthanon, Chiang Mai, Thailand	MG197752
<i>G (P.) mandarinus kimurai</i> (CM2–4)	Doi Inthanon, Chiang Mai, Thailand	MG197753
<i>G (P.) mandarinus kimurai</i> (CM5)	Doi Inthanon, Chiang Mai, Thailand	MG197754
<i>G (P.) mandarinus fangana</i> (CM1–3)	Doi Phu Meun, Chiang Mai, Thailand	MG197751
<i>G (P.) mandarinus stilwelli</i> (WX1)	Weixi, Yunnan, China	MG197755
<i>G (P.) mandarinus stilwelli</i> (YX1)	Yunxian, Yunnan, China	MG197755
<i>G (P.) mandarinus stilwelli</i> (TC1–2)	Tengchong, Yunnan, China	MG197755
<i>G (P.) mandarinus stilwelli</i> (YB1–2)	Yangbi, Yunnan, China	MG197755
<i>G (P.) mandarinus stilwelli</i> (SG1)	Tarung Hka River, Sagaing, Myanmar	MG197755
<i>G (P.) mandarinus stilwelli</i> (KC1)	Chudu Razi Hills, Kachin, Myanmar	MG197755
<i>G (P.) mandarinus mandarinus</i> (BX1–4)	Baoxing, Sichuan, China	MG197749
<i>G (P.) mandarinus mandarinus</i> (BX5)	Baoxing, Sichuan, China	MG197750

***Graphium (Pazala) wenlingae* Hu, Cotton & Monastyrskii sp. nov.**  
(Figure 3)

*Pazala glycerion*: Monastyrskii & Devyatkin, 2000: 473. C. Vietnam (Ngoc Linh)

*Graphium (Pazala) mandarinus* [partim]: Monastyrskii & Devyatkin, 2003: 12. C. Vietnam (to Lam Dong).

*Graphium (Pazala) mandarinus* [partim]: Monastyrskii, 2007: 96. C. Vietnam (to Lam Dong)  
*Graphium (Pazala) mandarinus* [partim]: Monastyrskii & Devyatkin, 2015: 15. C. Vietnam (to Kon Tum).

**Description:** Male: Forewing length: 29.5–32.0 mm (mean =  $31.2 \pm 1.44$  mm,  $n = 3$ ). Forewing triangulate, broad, apex not produced, termen slightly concave in the medium portion. Forewing upperside: white, the upper and outer 1/3 (mostly the discocellular, the subterminal, and the terminal areas) hyaline and glossy; 10 black bands lined from the humeral to the termen, among which the 1<sup>st</sup> to the 6<sup>th</sup> almost run parallel; the 1<sup>st</sup> and the 2<sup>nd</sup> bands reach the tornal margin, the 3<sup>rd</sup> to the 5<sup>th</sup> bands extend beyond the discal cell and abut up the base of veins CuA<sub>2</sub>, CuA<sub>1</sub>, and M<sub>3</sub>, the 6<sup>th</sup> band at the end of cell, often connected with the 5<sup>th</sup> band by a transverse black fine line, the 7<sup>th</sup> band joins the 8<sup>th</sup> band just at vein M<sub>2</sub>, extends to the tornus and joins the 9<sup>th</sup> band at vein CuA<sub>2</sub> or just below it in cell CuA<sub>2</sub>, the 9<sup>th</sup> band curved inward in cell R<sub>4</sub>, the 10<sup>th</sup> band independent, extending from the apex to vein CuA<sub>2</sub> or just below it in cell CuA<sub>2</sub>; the veins CuA<sub>1</sub> to R<sub>4+5</sub> are black after meeting the 6<sup>th</sup> and 7<sup>th</sup> bands and then divide the whitish-hyaline areas between the 6<sup>th</sup> to 10<sup>th</sup> bands into spots. Forewing underside: colour and markings as upperside, but the hyaline areas are glossier. Hindwing narrow triangulate in general, costa very oblique, vein M<sub>3</sub> extends into a sword-like tail, termen slightly dented at the end of veins, the end of cells CuA<sub>1</sub> to M<sub>1</sub> scalloped. Hindwing upperside: white with long white hair covering the inner 1/3; tornal margin without any black, a large brown androconial patch near the humeral, a black sub-basal band extends from the costal along the lower cellular vein and ends at the base of vein CuA<sub>2</sub>, while the remaining bands visible from underside, two obliquely neighbouring yellow tornal spots encircled by black lines, with a small greyish blue spot below; the discal bands completely absent but visible from the underside; the submarginal black band coupled and interrupted by veins M<sub>1</sub> and Rs, reaching cell R<sub>5</sub> or M<sub>1</sub>, with the inner bands fainter; the terminal band single, also interrupted by veins M<sub>1</sub> and Rs, reaching cell R<sub>5</sub> or R<sub>i</sub>; all black bands, except the sub-basal one, join in the black area at the end of cells CuA<sub>1</sub> to M<sub>2</sub>, with a greyish-blue lunule in each cell; tail black with white tip. Hindwing underside: colour and markings similar to upperside but with a pale yellow hue, all black bands and markings better defined, especially the basal, sub-basal, and discal bands, two discal black lines twisting into an “8”-shaped pattern, with both rings white or just a rather faint yellow tinge in the upper ring, the edge of the lower ring extends along veins CuA<sub>1</sub> to M<sub>1</sub>; a square creamy white spot above each greyish-blue lunule in the tornal area, the yellow spots at the tornus reduced and crowned by fine white lines.

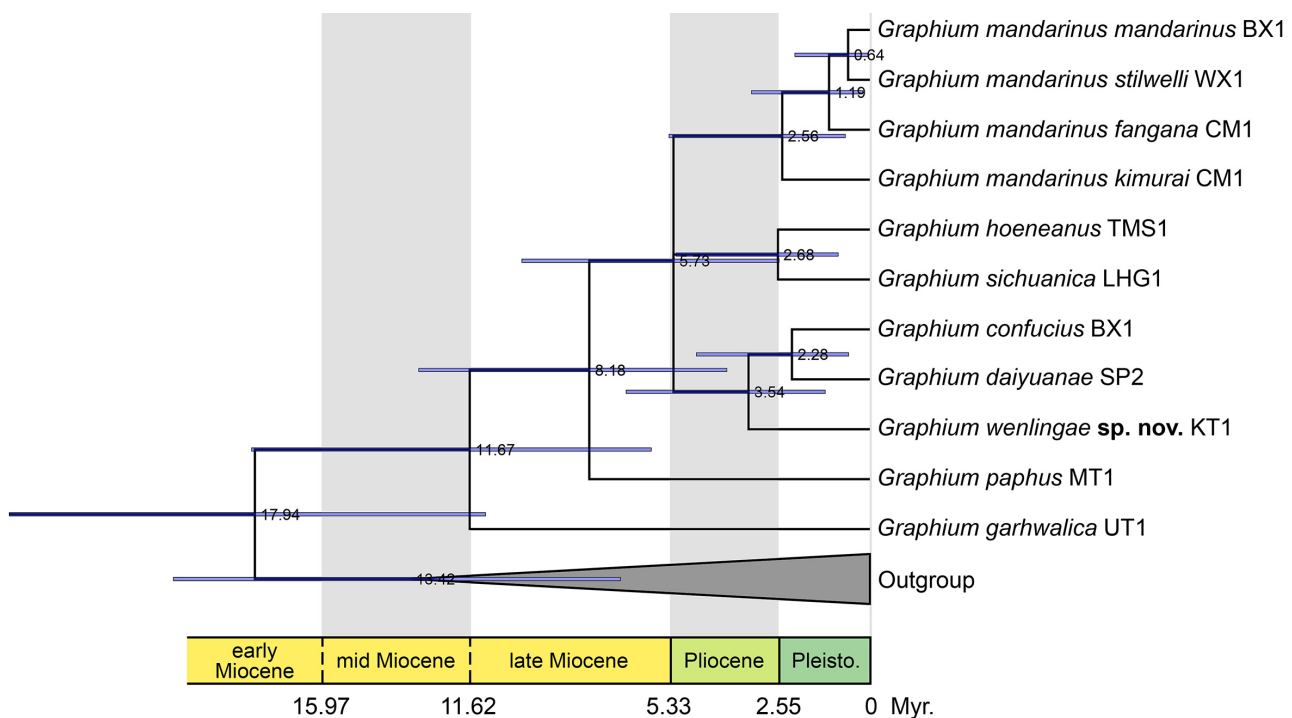


**FIGURE 2.** Bayesian molecular dating for species and subspecies in the *Graphium (Pazala) mandarinus* group, with outgroups collapsed. Values at nodes indicate the median divergence times, purple bars show 95% CI. Pleisto. = Pleistocene.

Female: Only two females were available. Forewing lengths of both specimens 34.0 mm. General appearance similar to male but larger and even paler. The 4<sup>th</sup> black band on the forewing not reduced.

Male genitalia (Figure 4): Two males were dissected, and found to be largely similar except for variation in the teeth of the medial harpe. Moderately sclerotised. Ring wavy in the upper half; saccus small; distance between the base of socii 0.40 mm ( $n = 2$ ). Valve oval in general, the dorsal terminal harpe with mostly straight edge and elongated acute tip; the edge of dorsal subterminal harpe almost touching the base of the tip of the dorsal terminal harpe; the medial harpe mostly straight, the dorsal projection bayonet-shaped with indented tip; a variable number of small teeth (1–2) occur in the middle of the medial harpe.

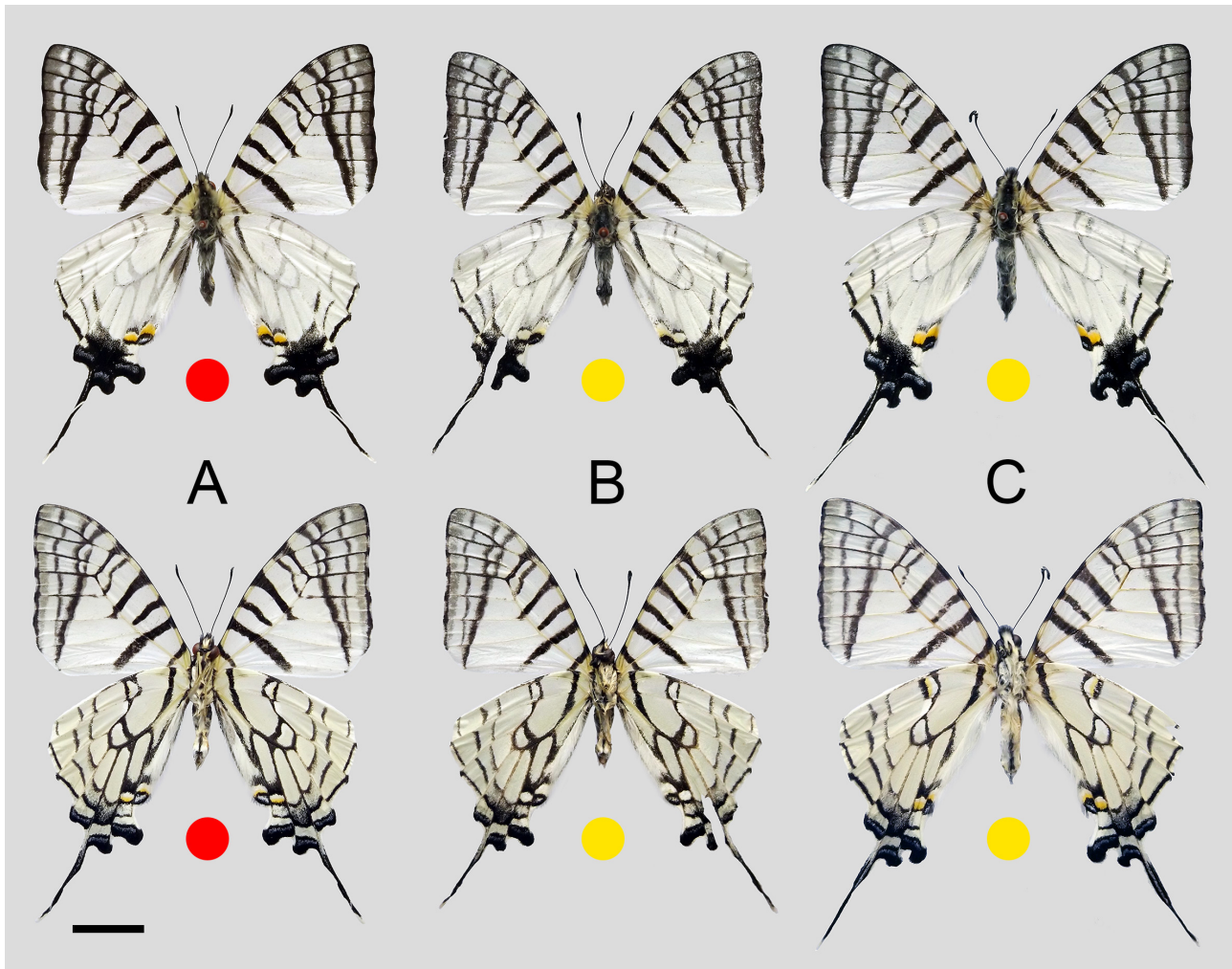


**FIGURE 3.** *Graphium (Pazala) wenlingae* Hu, Cotton & Monastyrskii sp. nov.; red dot: holotype, yellow dots: paratypes; upperside on the first row, underside on the second row; A–B: ♂, Ngoc Linh, Kon Tum, C. Vietnam; C: ♀, Tay Giang, Quang Nam, C. Vietnam; scale bar = 10 mm.

Female genitalia (Figure 5): Only one female was available for dissection. Lamella postvaginalis distinctly rounded; lamella antevaginalis broad in the ventral plane, lined with moderately sclerotised longitudinal striae; ostial lobe heavily sclerotised, broad at the base and gradually narrowed into a sharp tip in lateral view, while the posterior margin is deeply concave with a pair of acute spurs in ventral view.

Differential Diagnosis: The new species resembles *G. (P.) daiyuanae* Hu, Zhang & Cotton, 2018, *G. (P.) mandarinus kimurai* Murayama, 1982, *G. (P.) mandarinus fangana* (K. Okano, 1986), and *G. (P.) mandarinus stilwelli* Cotton & Hu, 2018 (Figure 6), but can be distinguished by careful examination of the following characters: 1) size smaller than *daiyuanae* and *mandarinus stilwelli*, similar to that of *mandarinus kimurai* and *mandarinus fangana*; 2) forewing termen not oblique outwardly from apex to tornus as in *daiyuanae* and female *mandarinus kimurai* and *mandarinus fangana* (a); 3) upperside hindwing rather paler, the basal, lower half of sub-

basal, and discal bands completely absent in both sexes (while commonly present in other taxa) (b); 4) both rings of the discal bands on the hindwing underside mostly white, except a very thin line of creamy yellow in the upper ring (c) (the upper ring typically yellow in other taxa); 5) the interspaces between coupled submarginal bands at cells  $M_3$  and  $M_2$  more irrigated with whitish scales than in other taxa (d).

**TABLE 2.** Monophylizer assessment of species and subspecies in the *Graphium (Pazala) mandarinus* group.

Taxon	Assessment	Tanglees
<i>G. (P.) garhwalica</i>	monophyletic	-
<i>G. (P.) paphus</i>	monophyletic	-
<i>G. (P.) sichuanica</i>	monophyletic	-
<i>G. (P.) hoeneanus</i>	monophyletic	-
<i>G. (P.) wenlingae</i> sp. nov.	monophyletic	-
<i>G. (P.) daiyuanae</i>	monophyletic	-
<i>G. (P.) confucius</i>	monophyletic	-
<i>G. (P.) mandarinus</i>	monophyletic	-
ssp. <i>kimurai</i>	monophyletic	-
ssp. <i>fangana</i>	monophyletic	-
ssp. <i>stilwelli</i>	paraphyletic	ssp. <i>mandarinus</i> , ssp. <i>fangana</i>
ssp. <i>mandarinus</i>	monophyletic	-

**TABLE 3.** The Kimura 2-parameter distances (shown in percentages) between taxa in *Graphium (Pazala) mandarinus* group, including *G. (P.) wenlingae* Hu, Cotton & Monastyrskii sp. nov.

Taxon	1	2	3	4	5	6	7	8a	8b	8c	8d
1. <i>garhwalica</i>											
2. <i>paphus</i>	5.42										
3. <i>sichuanica</i>	4.85	5.07									
4. <i>hoeneanus</i>	5.08	4.81	2.04								
5. <i>wenlingae</i> sp. nov.	4.81	4.83	2.79	3.47							
6. <i>daiyuanae</i>	4.54	5.32	3.98	3.42	2.38						
7. <i>confucius</i>	5.27	5.12	4.16	4.09	2.24	1.71					
8a. <i>mandarinus kimurai</i>	6.20	5.72	4.01	4.17	3.78	3.88	3.41				
8b. <i>mandarinus fangana</i>	5.76	5.96	3.39	4.11	3.03	3.46	2.67	1.64			
8c. <i>mandarinus stilwelli</i>	5.93	6.13	3.55	4.28	3.19	3.62	3.12	1.48	0.46		
8d. <i>mandarinus mandarinus</i>	6.48	6.33	4.01	4.43	3.38	3.22	2.99	1.67	0.95	0.49	

In male genitalia, the tip of dorsal terminal harpe acute and elongated (short in *mandarinus* and *daiyuanae*), dorsal subterminal harpe large, joining dorsal terminal harpe and forming a triangle, dorsal projection bayonet-shaped (Figure 4), distance between the base of socii 0.40 mm. In female genitalia the ostial lobe forming a large up-curving spur in lateral view, the posterior margin deeply concave with a pair of acute spurs in ventral view (Figure 5).

**Type Material: Holotype:** VIETNAM: ♂, Ngoc Linh National Park (15°07.432' N, 107°59.915' E; 2,416 m), Kon Tum Province, 2018–IV, D. N. Vang leg. [KIZ, 0101805].

**Paratypes:** VIETNAM: 1♂, Ngoc Linh National Park (1,800 m), Kon Tum Province, 1998–IV–3, A. Monastyrskii leg. [VFM]; 1♀, ditto (1,600 m), 1998–IV–5, A. Monastyrskii leg. [VFM]; 1♂, same collecting data as holotype [SJH]; 1♀, Tay Giang (1,300 m), Quang Nam Province, 2017–IV, L. T. Le leg. [KIZ, 0101806].

The holotype and one paratype were deposited in Kunming Institute of Zoology (KIZ), Chinese Academy of Sciences (Li *et al.* 2015).

**Distribution:** The new species is currently known only from Kon Tum plateau of Truong Son (Annamite) Range in C. Vietnam (Quang Nam and Kon Tum Provinces). We can also expect to discover this species in adjacent Gia Lai Province (e.g. Kon Ka Kinh National Park) and in Lam Dong Province (e.g. Bi Doup Nui Ba and Chu Yang Sin National Parks).

**Phenology:** Likely univoltine. All specimens in this study were collected in April.

**Host plant:** Unknown, presumably a plant species belonging to family Lauraceae representatives of which (e.g. genera *Neolitsea*, *Machilus*, *Cinnamomum*, and *Persea*) are host plants of such relatives as *Graphium (Pazala) eurous* and *G. (P.) mullah* (Igarashi & Fukuda 2000).

**Derivatio nominis:** The specific name of this elusive new taxon was dedicated to Dr. Wen-Ling Wang, a very close friend of the first author. The species name is to be treated as a noun in apposition.

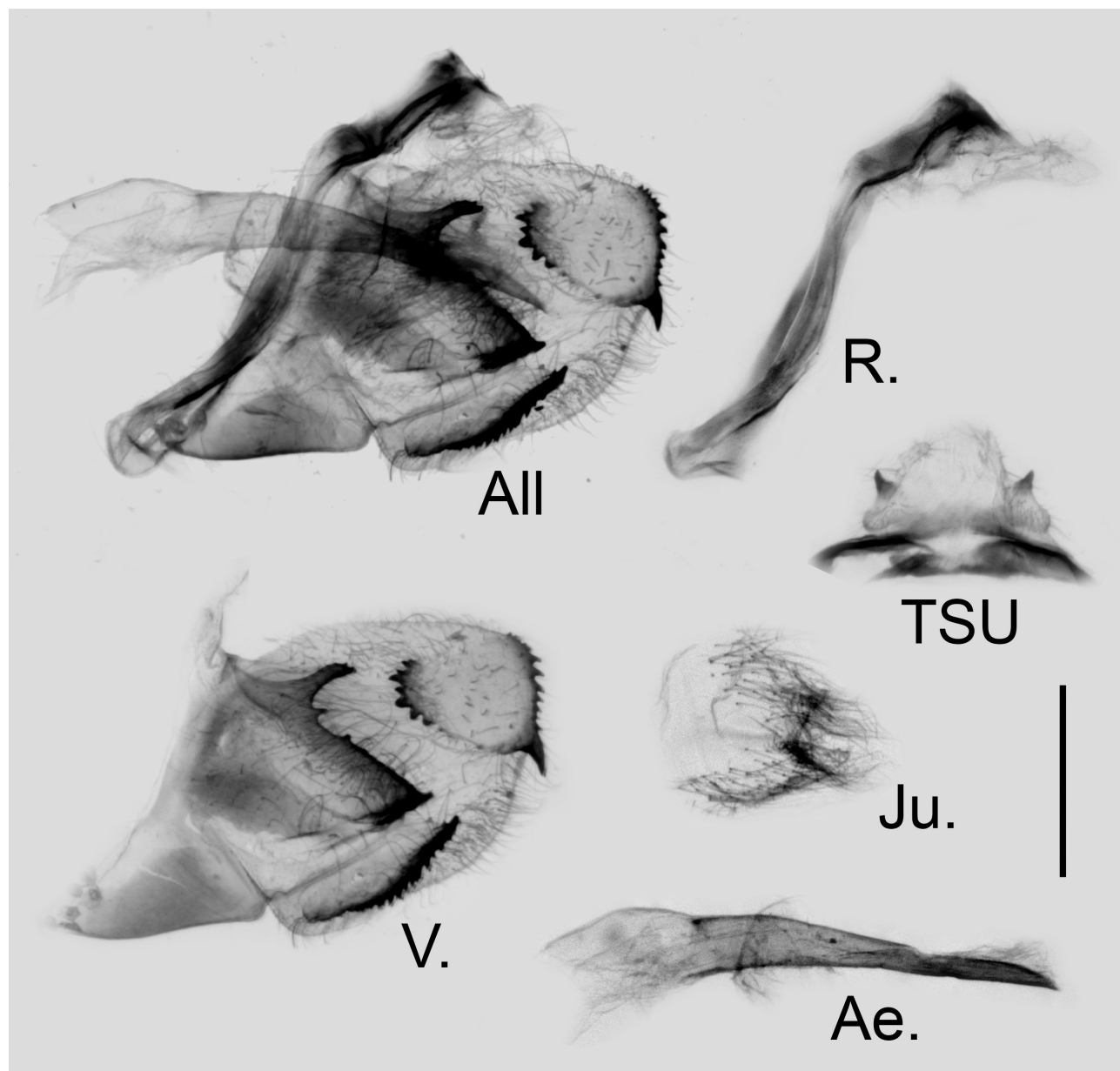


**FIGURE 4.** Male genitalia of *Graphium (Pazala) wenlingae* Hu, Cotton & Monastyrskii sp. nov. from Ngoc Linh, Kon Tum, C. Vietnam; scale bar = 1.0 mm. All: genitalia as a whole, R.: lateral view of ring, TSU: dorsal view of tegumen, socii, and uncus, V. right valve, Ae.: lateral view of aedeagus, Ju.: ventral view of juxta.



**FIGURE 5.** Female genitalia of *Graphium (Pazala) wenlingae* Hu, Cotton & Monastyrskii sp. nov. from Tay Giang, Quang Nam, C. Vietnam; lateral view above, ventral view below; scale bar = 1.0 mm.

#### Key to taxa of the *G. (P.) mandarinus* group based on wing pattern

- |   |                                                                                                                       |                              |
|---|-----------------------------------------------------------------------------------------------------------------------|------------------------------|
| 1 | Hindwing underside with distinct 8-shaped discal band .....                                                           | 2                            |
| - | 8-shaped band indistinct, discal band almost single and straight .....                                                | 10                           |
| 2 | Forewing apex produced, usually larger in size, with prominent black bands and bright yellow markings .....           | <i>confucius</i>             |
| - | Forewing apex not produced, smaller in size .....                                                                     | 3                            |
| 3 | Middle of forewing termen distinctly concave .....                                                                    | <i>paphus</i>                |
| - | Middle of forewing termen not concave .....                                                                           | 4                            |
| 4 | Base of forewing veins CuA <sub>2</sub> and CuA <sub>1</sub> white .....                                              | <i>garhwalica</i>            |
| - | Base of these veins (at least CuA <sub>1</sub> ) black .....                                                          | 5                            |
| 5 | Forewing termen distinctly inwardly oblique from tornus to apex .....                                                 | 6                            |
| - | Forewing termen indistinctly angled inwards to apex .....                                                             | 7                            |
| 6 | Basal band on hindwing upperside usually complete, yellow markings on the underside brighter .....                    | <i>daiyuanae</i>             |
| - | Basal band on hindwing upperside incomplete, yellow markings on the underside rather pale .....                       | <i>wenlingae</i> sp. nov.    |
| 7 | Larger and darker, basal band on hindwing upperside complete, discal band on hindwing upperside usually present ..... | <i>mandarinus mandarinus</i> |

-	Paler, basal band on the hindwing upperside usually incomplete.....	8
8	Medium sized, discal band on hindwing upperside incomplete, only with a trace above the discocell.....	<i>mandarinus stilwelli</i>
-	Smaller, discal band on hindwing upperside absent .....	9
9	Base of forewing vein CuA <sub>1</sub> black .....	<i>mandarinus fangana</i>
-	Base of forewing vein CuA <sub>1</sub> white .....	<i>mandarinus kimurai</i>
10	Smaller and darker, 9 <sup>th</sup> forewing band reaches the tornus, hindwing subterminal band continuous.....	<i>sichuanica</i>
-	Larger and paler, 9 <sup>th</sup> forewing band not reaching the tornus, hindwing subterminal band interrupted.....	<i>hoeneanus</i>

## Discussion

The discovery of *G. (P.) wenlingae* sp. nov. increases the total number of members of the *mandarinus* group to eight species. Three of them are distributed in northern and central parts of Vietnam (Figure 7); however, the current work is not the first publication to record their distribution in the country. Monastyrskii & Devyatkin (2015) had already collated records of *Graphium mandarinus* (Oberthür, 1879) from N. Vietnam (Lao Cai and Ha Giang Provinces) and C. Vietnam (Kon Tum Province). Based on our previous work (Hu *et al.*, 2018) and the current study, three separate species were previously recorded in Vietnam under the name ‘*mandarinus*’. These three species are *G. (P.) confucius* from Lao Cai and Ha Giang Provinces, *G. (P.) daiyuanae* from Lao Cai Province and *G. (P.) wenlingae* sp. nov. from Kon Tum and Quang Nam Provinces. The high species richness of the *mandarinus* group in Indochina is not an unexpected fact. A number of other representatives of Sino-Himalayan butterfly fauna have previously been found in Vietnam (Monastyrskii 2010). The Truong Son (Annamite) Range, extending for nearly 1,200 km from north to south along the Vietnamese border with Laos and Cambodia is a rather poorly studied area of butterfly endemism (Monastyrskii & Holloway 2013). For *Pazala*, a complex group, the species/subspecies richness, geographic distribution and endemism in this area would be intriguing topics to study further. This area represents a new range extension for this once-believed Palaearctic subgenus of *Graphium*. Answering these aspects would greatly complement our understanding of *Pazala*, and eventually benefit the modern taxonomy of *Graphium*, as recommended by Smith (2005).

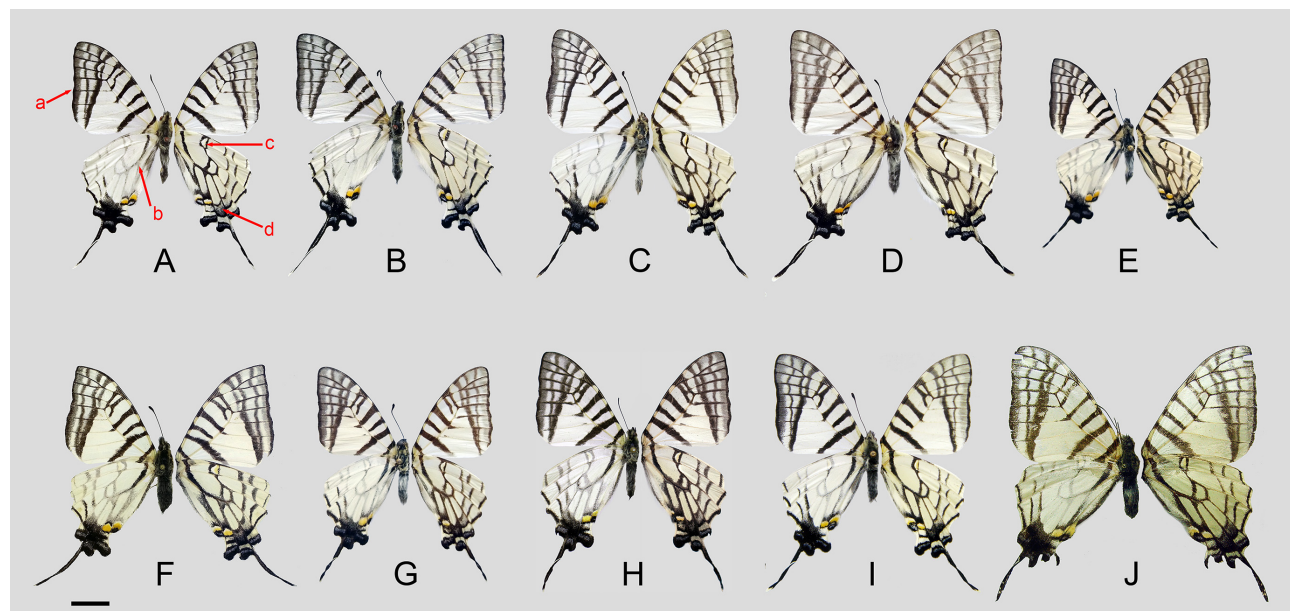


**FIGURE 6.** Differential diagnoses of *Graphium (Pazala) wenlingae* Hu, Cotton & Monastyrskii sp. nov. (A: ♂, B: ♀) and similar taxa, upperside on the left half, underside on the right half; C: *G. (P.) daiyuanae* Hu, Zhang & Cotton, 2018, ♂; D: ditto, ♀; E: *G. (P.) mandarinus kimurai* Murayama, 1982, ♂; F: ditto, ♀; G: *G. (P.) mandarinus fangana* (K. Okano, 1986), ♂; H: ditto, ♀; I: *G. (P.) mandarinus stilwelli* Cotton & Hu, 2018, ♂; J: ditto, ♀ © Zoologisches Forschungsinstitut und Museum Alexander Koenig (ZFMK), Bonn, Germany; scale bar = 10 mm.

Currently *G. (P.) wenlingae* sp. nov. is only known from the restricted area of the Kon Tum plateau in the central part of the Truong Son Range. This is isolated by a central section of relatively low hills from the mountains of northern Truong Son. The gap between the ranges of *G. (P.) wenlingae* sp. nov. and both *G. (P.) daiyuanae* and *G.*

(*P.*) *confucius*, where no taxa in the *mandarinus* group have yet been recorded, is about 950 km. There may potentially be habitat for one or more of these *mandarinus* group species in this region.

The Truong Son Range consists of very old mountains formed in the Paleozoic and Mesozoic epochs (Averyanov *et al.* 2003), long before the mid Pliocene to early Pleistocene when the divergence of *G. (P.) wenlingae* sp. nov. occurred, according to our molecular dating analysis (Figure 2). During this period, with the climate cooling down in an oscillating pattern (Zachos *et al.* 2001) and eventually reaching the last glacial maximum (LGM) globally, the low-altitude river valleys gradually played the role of refugial shelters for animals in the cold periods of climate oscillation (Stewart & Lister 2001; Keppel *et al.* 2012). After each cold period, with the increase in temperature when the climate entered the next warm period, plausibly many species would have again retreated to higher altitudes into cooler habitats. Such cyclical repeated movements driven by climate oscillation are widely accepted as a vicariance driver in Indochina, especially along the Truong Son Range (Woodruff 2010; Kong *et al.* 2017). Our molecular dating analysis showed that *G. (P.) wenlingae* sp. nov. split before *G. (P.) daiyuanae* + *G. (P.) confucius*, which can probably be attributed to the quicker warming up in the southern part of Vietnam compared to the North in each oscillating cycle.

A similar hypothesis may also be applied to the *G. (P.) sichuanica* + *G. (P.) hoeneanus* clade and the entire *G. (P.) mandarinus* clade, which occupies the eastern margin of the Hengduan Mountains to various hills in S. to S.E. China, and the southern margin of the Hengduan Mountains to the Shan Highlands (Figure 7), where climate oscillation in the Pliocene to Pleistocene also prevailed (Zachos *et al.* 2001). The trichotomy in our molecular dating analysis, the low support values for those nodes, as well as very similar external and genitalic morphology all suggested a fast divergence between lineages.

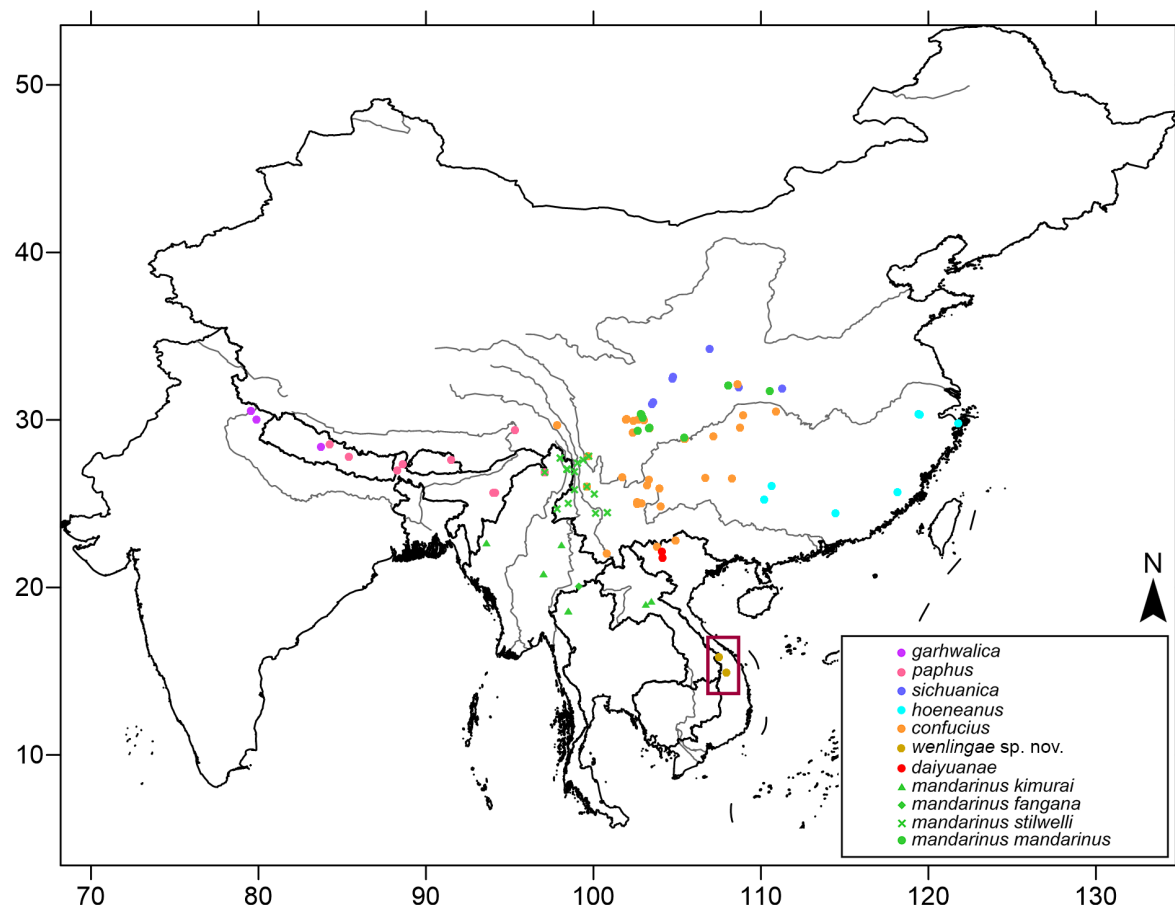


**FIGURE 7.** Distribution map of the *Graphium (Pazala)* *mandarinus* group, with the distribution of *G. (P.) wenlingae* sp. nov. highlighted in a red box.

## Acknowledgements

We thank R. I. Vane-Wright, T. Racheli, and an anonymous reviewer for providing very useful comments on the manuscript. This study was funded by the NSFC Programme of China (41761011) and the Biodiversity Conservation Programme of the Ministry of Ecology and Environment, China (China-BON Butterflies) (SDZXWJZ01013).

## References

- Averyanov, L.V., Phan, K.L., Nguyen, T.H. & Harder, D.K. (2003) Phylogenetic review of Vietnam and adjacent areas of eastern Indochina. *Komarovia*, 3, 1–83.
- Ayres, D.L., Darling, A., Zwickl, D.J., Beerli, P., Holder, M.T., Lewis, P.O., Huelsenbeck, J.P., Ronquist, F., Swofford, D.L., Cummings, M.P., Rambaut, A. & Suchard, M.A. (2012) BEAGLE: an application programming interface and high-performance computing library for statistical phylogenetics. *Systematic Biology*, 61, 170–173.  
<https://doi.org/10.1093/sysbio/syr100>
- Bertheau, C., Schuler, H., Krumböck, S., Arthofer, W. & Stauffer, C. (2011) Hit or miss in phylogenetic analyses: the case of the cryptic NUMTs. *Molecular Ecology Resources*, 11, 1056–1059.  
<https://doi.org/10.1111/j.1755-0998.2011.03050.x>
- Condamine, F.L., Sperling, F.A.H., Wahlberg, N., Rasplus, J.-Y. & Kergoat, G.J. (2012) What causes latitudinal gradients in species diversity? Evolutionary processes and ecological constraints on swallowtail biodiversity. *Ecology Letters*, 15, 267–277.  
<https://doi.org/10.1111/j.1461-0248.2011.01737.x>
- Folmer, O., Black, M.B., Hoch, W., Lutz, R.A. & Vrijehock, R.C. (1994) DNA primers for amplification of mitochondrial cytochrome c oxidase subunit I from diverse metazoan invertebrates. *Molecular Marine Biology and Biotechnology*, 3, 294–299.
- Hall, T.A. (1999) BioEdit: a user-friendly biological sequence alignment editor and analysis program for Windows 95/98/NT. *Nucleic Acids Symposium Series*, 41, 95–98.
- Hu, S.J., Cotton, A.M., Condamine, F.L., Duan, K., Wang, R.J., Hsu, Y.F., Zhang, X. & Cao, J. (2018) Revision of *Pazala* Moore, 1888: the *Graphium* (*Pazala*) *mandarinus* (Oberthür, 1879) group, with treatments of known taxa and descriptions of new species and new subspecies (Lepidoptera: Papilionidae). *Zootaxa*, 4441, 401–446.  
<https://doi.org/10.11646/zootaxa.4441.3.1>
- Huelsenbeck, J.P., Larget, B. & Alfaro, M.E. (2004) Bayesian phylogenetic model selection using reversible jump Markov Chain Monte Carlo. *Molecular Biology and Evolution*, 21, 1123–1133.  
<https://doi.org/10.1093/molbev/msh123>
- Igarashi, S. & Fukuda, H. (2000) *The Life Histories of Asian Butterflies. II*. Univ. Press, Tokyo, 711 pp..
- Keppel, G., Van Niel, K.P., Wardell-Johnson, G.W., Yates, C.J., Byrne, M., Mucina, L., Schut, A.G.T., Hopper, S.D. & Franklin, S.E. (2012) Refugia: identifying and understanding safe havens for biodiversity under climate change. *Global Ecology and Biogeography*, 21, 393–404.  
<https://doi.org/10.1111/j.1466-8238.2011.00686.x>
- Kimura, M. (1980) A simple method for estimating evolutionary rates of base substitutions through comparative studies of nucleotide sequences. *Journal of Molecular Evolution*, 16, 111–120.  
<https://doi.org/10.1007/BF01731581>
- Koiwaya, S. (1993) Description of three new genera, eleven new species and seven new subspecies of butterflies from China. *Studies of Chinese Butterflies*, 2, 43–111, pls. 9–27. [in Japanese with English descriptions]
- Kong, H.L., Condamine, F.L., Harris, A.J., Chen, J.L., Pan, B., Möller, M., Hoang, V.S. & Kang, M. (2017) Both temperature fluctuations and East Asian monsoons have driven plant diversification in the karst ecosystems from southern China. *Molecular Ecology*, 26, 6414–6429.  
<https://doi.org/10.1111/mec.14367>
- Lanfear, R., Frandsen, P.B., Wright, A.M., Senfeld, T. & Calcott, B. (2017) PartitionFinder 2: new methods for selecting partitioned models of evolution for molecular and morphological phylogenetic analyses. *Molecular Biology and Evolution*, 34, 772–773.  
<https://doi.org/10.1093/molbev/msw260>
- Lepage, T., Bryant, D., Philippe, H. & Lartillot, N. (2007) A general comparison of relaxed molecular clock models. *Molecular Biology and Evolution*, 24, 2669–2680.  
<https://doi.org/10.1093/molbev/msm193>
- Li, K.Q., Wang, Y.Z., Dong, D.Z. & Zhang, L.K. (2015) Catalog of insect type specimens preserved at the Kunming Institute of Zoology, Chinese Academy of Science with corrections of some specimens. *Zoological Research*, 36, 263–284.  
<https://doi.org/10.13918/j.issn.2095-8137.2015.5.263>
- Miller, M.A., Schwartz, T., Pickett, B.E., He, S., Klem, E.B., Scheuermann, R.H., Passarotti, M., Kaufman, S. & O’Leary, M.A.

- (2015) A RESTful API for access to phylogenetic tools via the CIPRES science gateway. *Evolutionary Bioinformatics Online*, 11, 43–48.  
<https://doi.org/10.4137/EBO.S21501>
- Minh, B.Q., Nguyen, M.A.T. & von Haeseler, A. (2013) Ultrafast approximation for phylogenetic bootstrap. *Molecular Biology and Evolution*, 30, 1188–1195.  
<https://doi.org/10.1093/molbev/mst024>
- Monastyrskii, A.L. (2007) *Butterflies of Vietnam. Papilionidae. Vol. 2*. Dolphin Media, 158 pp.
- Monastyrskii, A.L. (2010) On the origin of the recent fauna of butterflies (Lepidoptera, Rhopalocera) of Vietnam. *Entomology Review*, 90, 39–58.  
<https://doi.org/10.1134/S0013873810010045>
- Monastyrskii, A.L. & Devyatkin, A.L. (2000) New taxa and new records of butterflies from Vietnam (Lepidoptera, Rhopalocera). *Atalanta*, 31 (3/4), 471–492.
- Monastyrskii, A.L. & Devyatkin, A.L. (2003) *Butterflies of Vietnam (an Illustrated checklist)*. Thong Nhat Printing House, 56 pp., 14 pls.
- Monastyrskii, A.L. & Holloway, J.D. (2013) Chapter 5. The Biogeography of the Butterfly Fauna of Vietnam With a Focus on the Endemic Species (Lepidoptera). In: Sivia-Opps, M. (Ed.), *Current Progress in Biological Research*. IntechOpen, Rijeka, pp. 95–123.
- Monastyrskii, A.L. & Devyatkin, A.L. (2015) *Butterflies of Vietnam (An Illustrated Checklist)*. 2<sup>nd</sup> Edition. Planorama Media Co., Ltd., Hanoi, 59 pp.
- Mutanen, M., Kivelä, S.M., Vos, R.A., Doorenweerd, C., Ratnasingham, S., Hausmann, A., Huemer, P., Dincă, V., van Niekerken, E.J., Lopez-Vaamonde, C., Vila, R., Aarvik, L., Decaëns, T., Efetov, K.A., Hebert, P.D.N., Johnsen, A., Karsholt O., Pentinsaari, M., Rougerie, R., Segerer, A., Tarmann, G., Zahiri, R. & Godfray, H.C.J. (2016) Species-level para- and polyphyly in DNA barcode gene trees: strong operational bias in European Lepidoptera. *Systematic Biology*, 65, 1024–1040.  
<https://doi.org/10.1093/sysbio/syw044>
- Nguyen, L.T., Schmidt, H.A., von Haeseler, A. & Minh, B.Q. (2015) IQ-TREE: a fast and effective stochastic algorithm for estimating maximum-likelihood phylogenies. *Molecular Biology and Evolution*, 32, 268–274.  
<https://doi.org/10.1093/molbev/msu300>
- O'Neill, S.L., Giordano, R., Colbert, A.M.E., Karr, T.L. & Robertson, H.M. (1992) 16S rRNA phylogenetic analysis of the bacterial endosymbionts associated with cytoplasmic incompatibility in insects. *Proceedings of the National Academy of Sciences of the United States of America*, 89, 2699–2702.  
<https://doi.org/10.1073/pnas.89.7.2699>
- Racheli, T. & Cotton, A.M. (2009) *Guide to the Butterflies of the Palearctic Region. Papilionidae. Part I*. Milano, Omnes Artes, 70 pp.
- Rehm, P., Borner, J., Meusemann, K., von Reumont, B.M., Simon, S., Hadrys, H., Misof, B. & Burmester, T. (2011) Dating the arthropod tree based on large-scale transcriptome data. *Molecular Phylogenetics and Evolution*, 61, 880–887.  
<https://doi.org/10.1016/j.ympev.2011.09.003>
- Ronquist, F., Teslenko, M., Van Der Mark, P., Ayres, D.L., Darling, A., Höhna, S., Larget, B., Liu, L., Suchard, M.A. & Huelsenbeck, J.P. (2012) MrBayes 3.2: efficient Bayesian phylogenetic inference and model choice across a large model space. *Systematic Biology*, 61, 539–542.  
<https://doi.org/10.1093/sysbio/sys029>
- Schenk, J.J. (2016) Consequences of secondary calibrations on divergence time estimates. *PLoS ONE*, 11, e0148228.  
<https://doi.org/10.1371/journal.pone.0148228>
- Smith, C.R. (2005) Why we are studying Oriental *Graphium* (Lepidoptera: Papilionidae) at the Natural History Museum, London. In: Yata, O. (Ed.), *A Report on Insect Inventory Project in Tropic Asia (TAIIV) "Network construction for the establishment of insect inventory in Tropic Asia (TAIIV)"*. Kyushu University, Fukuoka, pp. 49–56.
- Smith, C.R. & Vane-Wright, R.I. (2001) A review of the Afrotropical species of the genus *Graphium* (Lepidoptera: Rhopalocera: Papilionidae). *Bulletin of the British Museum (Natural History) Entomology*, 70, 503–719.
- Song, H., Buhay, J.E., Whiting, M.F. & Crandall, K.A. (2008) Many species in one: DNA barcoding overestimates the number of species when nuclear mitochondrial pseudogenes are coamplified. *Proceedings of the National Academy of Sciences of the United States of America*, 105, 13486–13491.  
<https://doi.org/10.1073/pnas.0803076105>
- Stewart, J.R. & Lister, A.M. (2001) Cryptic northern refugia and the origins of the modern biota. *TRENDS in Ecology & Evolution*, 16, 608–613.  
[https://doi.org/10.1016/s0169-5347\(01\)02338-2](https://doi.org/10.1016/s0169-5347(01)02338-2)
- Tamura, K., Stecher, G., Peterson, D., Filipski, A. & Kumar, S. (2013) MEGA6: Molecular evolutionary genetics analysis version 6.0. *Molecular Biology and Evolution*, 30, 2725–2729.  
<https://doi.org/10.1093/molbev/mst197>
- Thompson, J.D., Higgins, D.G. & Gibson, T.J. (1994) CLUSTAL W: improving the sensitivity of progressive multiple sequence alignment through sequence weighting, position-specific gap penalties and weight matrix choice. *Nucleic Acids Research*, 22, 4673–4680.

- <https://doi.org/10.1093/nar/22.22.4673>
- Thorne, J.L. & Kishino, H. (2002) Divergence time and evolutionary rate estimation with multilocus data. *Systematic Biology*, 51, 689–702.  
<https://doi.org/10.1080/10635150290102456>
- Thorne, J.L., Kishino, H. & Painter, I.S. (1998) Estimating the rate of evolution of the rate of molecular evolution. *Molecular Biology and Evolution*, 15, 1647–1657.  
<https://doi.org/10.1093/oxfordjournals.molbev.a025892>
- Woodruff, D.S. (2010) Biogeography and conservation in Southeast Asia: how 2.7 million years of repeated environmental fluctuations affect today's patterns and the future of the remaining refugial-phase biodiversity. *Biodiversity Conservation*, 19, 919–941.  
<https://doi.org/10.1007/s10531-010-9783-3>
- Zachos, J., Pagani, M., Sloan, L., Thomas, E. & Billups, K. (2001) Trends, rhythms, and aberrations in global climate 65 Ma to present. *Science*, 292, 686–693.  
<https://doi.org/10.1126/science.1059412>